Renewable and Sustainable Energy Reviews 208 (2025) 115017

Contents lists available at ScienceDirect

Renewable and Sustainable Energy Reviews

journal homepage: www.elsevier.com/locate/rser

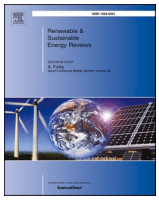

Computerized voltage reversal prevention in second and third year 1000-liter microbial fuel cell

Sunny Maye [a], Louis Delabays [b], Jules Sansonnens [a,c], Maxime Blatter [a], Gérald Huguenin [b], Fabian Fischer [a,d,*]

[a] Institute of Life Sciences, HES-SO Valais-Wallis, Rue de l'Industrie 19, 1950 Sion, Switzerland
[b] Embedded-Computing Systems, Haute-Ecole Arc, Rue de la Serre 7, 2610 St-Imier, Switzerland
[c] STEP de Châteauneuf, Avenue Maurice-Troillet 180, CP 2272, 1950 Sion, Switzerland
[d] Institute of Sustainable Energy, HES-SO Valais-Wallis, Rue de l'Industrie 23, 1950 Sion, Switzerland

ARTICLE INFO

Keywords:
Electronic
Digital
Data
Balancing
Automation
Healing

ABSTRACT

Large-scale microbial fuel cells treat wastewater while generating electricity, saving electricity and preventing air pollution. Long term use is difficult and hardly realized what is done in this work for more than three years. To prolong the time of service significantly a novel electronic control device was developed. It blocked the notorious and growing voltage reversals over time and balanced the 1000 L microbial fuel cell. It prevented voltage reversals in 64 units in a serial/parallel microbial fuel cell stack setup. This electronic voltage regulator worked in conjunction with maximum power point tracking. Both electronic tools individually optimized 16 microbial fuel cell units simultaneously to achieve stack balance and heal defiant units. To understand the applicability of this computational voltage reversal prevention controller, blocking experiments were performed with variable thresholds set at: +50, +25, 0, −25, −50 mV. The two best blocking thresholds were 50 mV and zero volts. The electronic balancing tool even revived the end-of-life 1000-L microbial fuel cell stack by resolving voltage reversals in the third year of constant operation. The voltage reversal blocker allowed to generate 1.7 to 2.7 times more power than without electronic control. The voltage balancing technique developed is expected to be useful for larger multi-unit microbial fuel cell stacks.

1. Introduction

Stacks of microbial fuel cells (MFCs) produce useable electricity [1] and represent a potential solution for next-generation water and wastewater treatment technologies [2]. For wastewater treatment, the research is well advanced but has not been applied [3]. Wastewater MFCs perform three additional tasks compared to the state of the art in wastewater treatment [4]. They purify wastewater while saving and generating electricity [5]. In addition, the technology prevents the release of volatile pollutants into the air [6], including carbon dioxide (CO_2), which is retained [7] and could be used to produce renewable fuels and chemicals [8].

Today, pilot-scale systems are being investigated at several sites, demonstrating the potential performance of larger systems which are reviewed in detail in Ref. [9] up to the 1000 L scale. A plug-flow reactor concept is proposed for the construction of large reactors to avoid unit-to-unit pumping [10] or the linear flow-through principle realized at the 1000 L scale [11]. However, the construction of large MFC stacks remains a challenge. After a relatively short period of time in use, unwanted deposits become visible, and a little later considerable deposits are possible [12]. In addition, continuous monitoring of the catalytic properties of the biofilm would be beneficial. Finally, the main challenge with serial MFC stacks is the frequent voltage reversals, which need to be avoided as they limit power generation [13].

A voltage reversal-free and well-balanced large MFC would be a breakthrough for the serial MFC stack approach [14]. Once such a system works, wastewater MFCs need to be compatible with existing sewer systems where wastewater flows vary because social and economic activities change constantly. In addition, rainwater infiltration sometimes dilutes chemical oxygen demand (COD) considerably [15]. Finally, municipalities (Canton of Valais, Switzerland) amortize the investment cost at 8 % per year, which refinances a new treatment plant by >50 % within 10 years. This means that future MFC stacks will have to remain in operation for 30 years, the minimum that can be expected from a current wastewater treatment plant. From a technological perspective,

* Corresponding author.
E-mail address: fabian.fischer@hevs.ch (F. Fischer).

https://doi.org/10.1016/j.rser.2024.115017
Received 19 March 2024; Received in revised form 16 October 2024; Accepted 17 October 2024

Nomenclature

Abbreviations

Cart	Trolley hosting a 250 L microbial fuel cell stack
COD	chemical oxygen demand
EESD	embedded electronic system device
GW	ground water
ISO	International Standards Organization
Line	four MFC-Units in parallel
MFC	microbial fuel cell
MFC-Line	parallel stack of four MFC-Units
MFC-Sub-Stack	serial stack of 250 L based four MFC-Lines
MFC-Unit	microbial fuel cell of 15.5 L process volume
MPPT	maximum power point tracker
OCV	open circuit voltage
PETG	polyethylene terephthalate glycol
p-OCV	pseudo-open circuit voltage
ppi	pores per inch
RPi	Raspberry Pi computer
RVC	reticulated vitreous carbon
Unit	shorter for MFC-Unit
WW	wastewater
WWTP	wastewater treatment plant

Symbols

$U_{MFC\text{-}Line}$	Voltage of four microbial fuel cell units interconnect in parallel
$U_{MFC\text{-}Sub\text{-}Stack}$	Voltage of four microbial fuel cell lines serially connected

electricity generation is the most discussed feature of MFCs, but the best energy production efficiency from wastewater is low, with 0.060 kWm^{-3} [11]. Nevertheless, several other studies have shown that electricity can be produced from serially stacked MFCs [1]. Stacked MFCs are proposed to be operated with electronic controls for easier operation [16]. Stack designs to improve voltage and power vary widely from 10 floating MFC in a stack [17] to 560 ceramic MFCs assembled in a 3D block fashion [18]. Model experiments with serial and parallel MFC stacks showed almost no difference in power output what is perfectly in line with theoretical expectations. However, serial stacking is from a pragmatic point of view preferred as voltages are higher with serial stacks and electronic devices available on the market are sold for such higher voltage output. This is the principal reason why in this work the serial arrangement is viewed and used as the preferred solution, while the simplest parallel stacking possible was integrated in the serial approach.

Energy savings are today far more significant with MFC technology than power generation. It saves 75 % of the electricity used in state-of-the-art medium sized WWTP [11]. The use of a maximum power point tracker (MPPT) with a serial MFC stack optimizes power generation, improves efficiency by enabling faster wastewater treatment [19]. Using power optimization electronics, operating voltages of around 0.1–0.4 V are possible for single MFC [20]. The use of multiple MFC units in serial connection is challenging because the voltages can easily be reversed [21]. The idea is to keep the voltage at a higher level to prevent reversals and increase performance. Higher single voltage MFCs are in fact capacitor-like MFCs. They even work without electrogens and produce in this case short-lived capacitive currents what is not wanted. Operating MFCs in capacitive mode without electrogens in wastewater treatment is not beneficial to the treatment process as it removes COD just slowly [22]. Therefore, electrogenic biofilms are important and the external load must be as low as possible to allow electrogens to exist what enables effective anaerobic respiration. In fact, with an MPPT the external resistance is higher than the internal resistance of the MFC units in a serial MFC stack, which is $<$ 50 Ohm/MFC. If the external load is minimized with an MPPT, it is likely that not all MFC units will have the same resistance. Minimal differences in resistance are expected even under unproblematic conditions. Voltage reversals have been shown to result from load mismatch [23]. A solution to avoid such reversals is to use one MPPT per every MFC unit [24]. Other means are electronic switches that establish balance between multiple MFC [25] units as shown for a small pilot algal MFC stack [26].

Electronic optimization seems possible, but process management should address all causes of voltage reversals. This includes inhomogeneous processing, which is likely in multi-unit MFC stacks. Voltage and other variations can occur in larger MFC stacks despite adherence to International Standards Organization (ISO) design norms [21]. Flux variations occur due to uneven particle deposits on the electrodes, in the connecting tubes and on the bottom of the reactor half-cells. It has been observed that reversals can recover without outside help [27]. Or they can be avoided by using double anodes [28], but in general the multiple anodes in MFC stacks should have similar or even identical properties [29], which is difficult to establish and maintain. One of the central measures to avoid are inhomogeneous fluxes over long periods of operation, MFC stacks require in this case repeated maintenance and therefore operator access to each MFC unit. This conflicts with the desire for a compact architecture to save space, as MFC treatment plants will require a lot of space if there is no other solution. The architecture for wastewater MFCs can be considered open, as wastewater is not very conductive. In addition, the flux rate is low and mixing for optimal kinetics is not an issue [30].

The most vulnerable element of a wastewater MFC is the anodic biofilm [31]. In wastewater treatment, the biofilm consists of a diverse community of microbes very similar to those found in municipal wastewater, there as planktonic microbes [32]. The taxonomic identification of these biofilm microbes at the species level is mostly not possible as they were never cultivated before [33]. Conversely, the main metabolism is often known at the genus level [34]. In addition to the electrogenic catalytic capacities of the biofilm, the electrode surface available for electrogene adhesion is another important kinetic parameter in MFCs [35]. Electrogenic biofilms are thin because the microbes breathe over the electrode surface. Therefore, it is required to use three dimensional (3D) electrodes such as reticulated vitreous carbon (RVC) [36] and others [37]. Nevertheless, porous anodes lose efficiency over time as bacteria, mineralized ionic solutes and particles deposit on the surface and fill the pores [38]. The compromised catalytic properties of the biofilm for electron donation can be monitored by polarization experiments or more sophisticated electrochemical analyses such as cyclic voltammetry [39], impedance spectroscopy and others. The data obtained can be processed using the Butler-Volmer-Monod equation [40] and others to determine exchange currents, source voltage, electron transfer mode, and internal resistances [41]. These data can be combined with microbial diversity analyses [42]. Another important process is cation migration across membranes, which is much slower than electron conduction through the external circuit and a significant hurdle for power generation.

Therefore, simple MFC stacks with low internal resistance are important for power generation [43]. Research shows two process approaches, a) focusing on power performance and b) maximizing purification. Both can be realized for example with a microbial fuel cell based on the idea of constructed wetlands [44], which is a novel variant of constructed wetlands for wastewater treatment that is still under research to integrate the bioelectric systems principle. It is in view of the current size of larger pilot MFCs a scale-up system that purifies

wastewater using the MFC approach to facilitate anaerobic respiration, digestion and power generation. Using this technology, strategies are being sought to avoid often observed clogging [2]. An alternative is the non-power generating scale-up MFC with short-circuit electrodes. It has enabled wastewater treatment at acceptable reaction rates [45]. Conversely, power generation with serial MFC stacks at this scale leads to unwanted voltage reversals and power generation is less efficient than the stack is capable of. Therefore, voltage reversal prevention needs to be solved, which will enable to focus more on the energy efficiency of large MFC stacks in future.

Various investigations have been carried out to understand how serial MFC stacks can be kept in balance without voltage reversals [46]. Indeed a number of practical methods were investigated but a satisfying solution is not achieved [47]. Voltage reversals seem to be more frequent and limiting than in most other battery-like systems, while adjustment measures as in other battery systems appear not that useful for MFC stacks. One of such controversial solutions is the application of bypass diodes that prevent voltage reversals [48]. Another approach is capacitor switches that force all MFC units to reach the same voltages [46]. About two years ago, a novel electronic voltage reversal blocking method was used to automatically prevent voltage reversals based on bioelectric processing data [26]. This electronic controller was combined with an MPPT to optimize four 3-L MFC units simultaneously. When the malfunctioning MFC unit was close to the start of a voltage reversal, it was disconnected from the MFC stack. The voltage status was checked 5 min later, and a decision was made to disconnect or reconnect. However, the electrogens were not guaranteed to execute constant breathing, which could lead to irreparable loss of electrogenic microbes in a typical MFC stack [42]. In this work, further research was carried out to enable reversal prevention while ensuring healing and constant respiration for electrogenic biofilms in any process situation.

In this work, a 1000-L MFC-Stack with 64 MFC-Units was to be controlled by a newly designed electronic voltage reversal controller/blocker in the second and third year of constant processing, something that was not performed before. It was designed to allow microbial anaerobic respiration in all process situations to support electrogenicity in biofilms. The controller was designed to prevent voltage reversals and balance this large MFC stack, which had been in operation for 16 months prior to this controlled work without voltage reversal regulation. The lost stack balance at this point was to be restored by the novel automated voltage reversal blocker. The computerized controller was set up to individually block voltage reversal in all 64 MFC units to achieve stack balance for best power generation. At the same time, the ability of a single MPPT to optimize 16 MFC units simultaneously, resulting in a balanced parallel/serial MFC stack, was investigated. The work then focused on finding the best voltage blocking thresholds for optimal power generation. Finally, the study aimed to balance the seemingly defiant overaged 1000-L MFC-Stack in its third year of operation what is the longest time such a large reactor has been operated any time before to the best of knowledge. It was then discussed whether this regulation technology could be proposed indeed for long-term use in wastewater treatment with MFCs.

2. Materials and methods

2.1. Construction and installation of the 1000-L microbial fuel cell stack

The 1000-L MFC-Stack was assembled from 64 MFC-Units made of polyethylene terephthalate glycol (PETG) modified polymer, the complete design is shown in Fig. 1 [11]. Each 16 L (15.5 L process volume) MFC-Unit consisted of two equally sized half-cells with four reticulated vitreous carbon (RVC, 100 ppi) electrodes per half-cell (ERG Aerospace Corporation, USA). A VANADion cation exchange membrane (IonPower, Germany) was fixed in between. The 12 m long MFC-Stack was organized into four MFC-Sub-Stacks (one per Cart 1–4), each 300 cm long and 61 cm wide. A top view with details can be seen in the center of

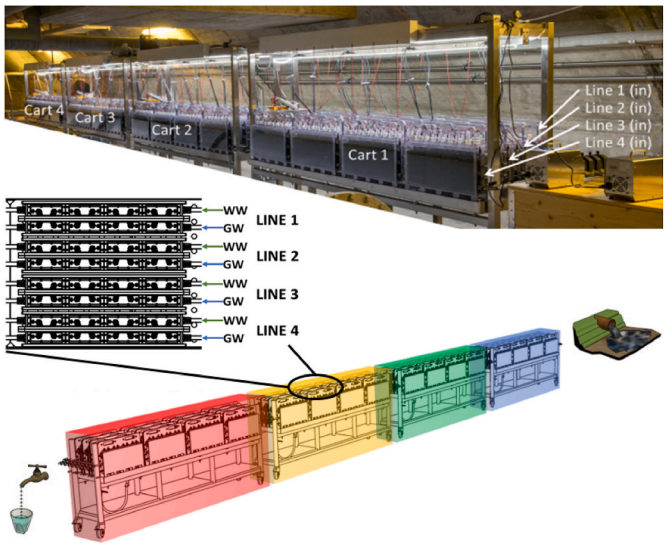

Fig. 1. Top: 1000-L MFC-Stack with 64 units at the Châteauneuf wastewater treatment plant (City of Sion, Switzerland). Middle: Top view on four MFC-Units (in Lines 1–4), four wastewater (WW) anodes and four cathodes with regulated oxygenated groundwater (GW). Bottom: 12 m long MFC-Stack divided into four electronically independent MFC-Sub-Stacks (red, yellow, green, blue).

Fig. 1.

The MFC-Stack was placed in an underground gallery of the Chateauneuf wastewater treatment plant (City of Sion, Switzerland). The temperatures of this facility, the MFC-Stack and the effluents were largely identical (between 10 °C in winter and 20 °C in summer). It was assumed that the effluents and catholytes flowed through the MFC-Stack by gravity. For experimental purposes, a constant hydraulic residence time was maintained by two four-channel pumps (BT100S-1, Golander Pump). The maximum capacity of the system to generate power and treat wastewater was 1 m^3/day. For this the wastewater influx had a global flow rate of 40 L/h or 10 L/h per anode channel (see Fig. 1, Lines 1–4 (in)). One of these channels among four MFC-Lines was 16 MFC-Units long (12 m) interconnected by tubes for effluent flux. In other words, the fresh wastewater was fed at MFC-Units 1,5,9,13 of Cart 1 and it passed then through all following 16 MFC Units of the respective Lines without new feed or release until it reached the last MFC-Units 4,8,12,16 of Cart 4 (for the Cart1-4 arrangement can be seen in Fig. 1). The catholyte was processed in the same manner using fresh ground water which was fed with a 10 times lower global flow rate of 4 L/h, what corresponded to 1 L/h per cathode channel (of 12 m length too).

2.2. Electric circuits, electronic voltage reversal blocking, and power tracking

The architecture of the MFC-Stack and the electronic circuits were designed in binary fashion to ensure compatibility with computer components. These comprised four maximum power point trackers, 64 electronic connection boards (one per MFC-Unit), two Raspberry Pi computers, four battery chargers, 16 polymer lithium batteries, various cables, circuit connection management electronics, Phyton programmed software and a central personal computer connected to the Internet (The assembly of all components is shown in Fig. 2).

A three-level concept hierarchy of electronic circuits was established. At the lowest level was the single MFC-Unit (see Fig. 2 for the MFC labels). It contained one anode and one cathode consisting of four RVC tiles per anode and per cathode which were wired in parallel to become one pseudo electrode. This was designed in this manner to ensure a stable MFC-Unit construction structure for long-term use. At the next higher level, four MFC-Units were electrically connected in parallel to

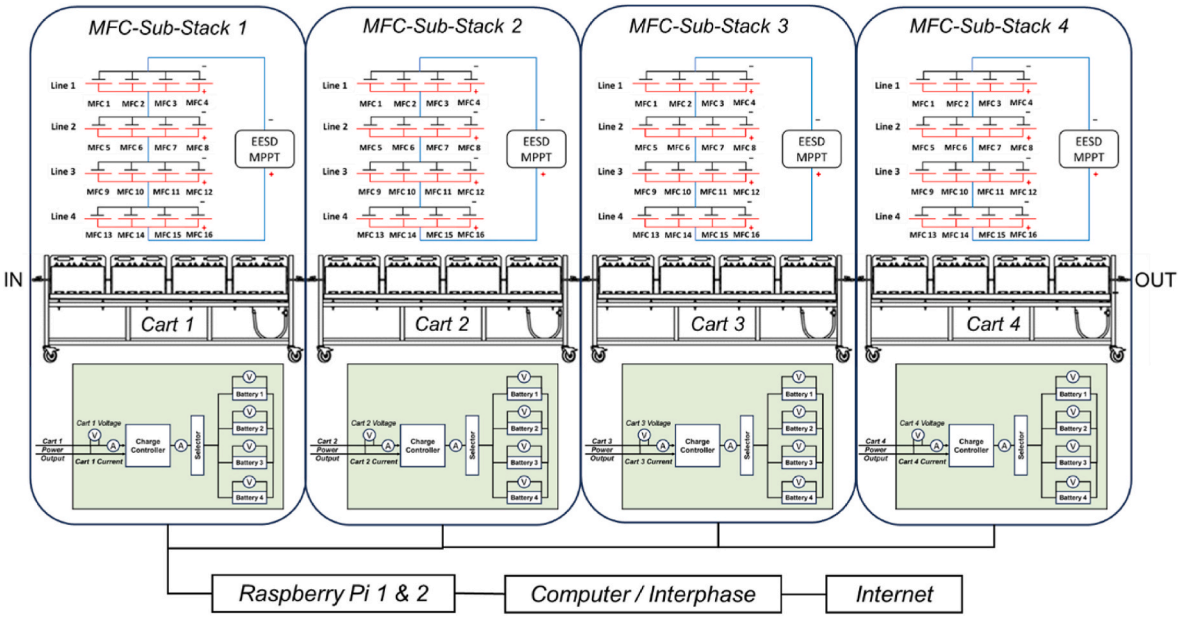

Fig. 2. General setup organization with electrical circuits and devices of the 1000-L MFC-Stack. Four parallel/serial MFC-Sub-Stacks connected with embedded electronic system devices (EESD) consisting of an MPPT and voltage regulator. The electronic power generation hierarchy consisted of three levels. Level 1: The single MFC-Unit was the first electronic level of the power generation circuit. Level 2: MFC-Lines consisted of four MFC-Units connected in parallel. Level 3: Four MFC-Lines in serial connection formed a serial stack circuit that produced useable electricity, here called MFC-Sub-Stack (Cart). Combination: Four MFC-Sub-Stacks formed the 1000-L MFC-Stack (Cart1-4). Bottom: detail about the charging electronics with four lithium polymer batteries per MFC-Sub-Stack (belonging to the EESD).

form a 3-m long MFC-Line (Fig. 1, look at the top view, which shows part of the MFC-Lines enlarged). Four of these MFC-Lines were connected in series to form an MFC-Sub-Stack (Cart) as the third level of electronic circuitry. Above this, the 1000-L MFC-Stack consisted of four MFC-Sub-Stacks, which did not share power generation circuits but did share the same control computer what is detailed in Fig. 2.

The MFC-Units were connected to two Raspberry Pi (RPi) computers via electronic circuit boards (one RPi for MFC-Stack process control, and the second RPi for energy harvesting and battery charging). The two RPi's interacted with the central computer, which served as the user interface, for parameter setting, process monitoring and data storage.

The Phyton software, coded in-house, managed the on/off switching of individual MFC-Units to and from the electrical circuits. A maximum power point tracker was added to the circuit of each MFC-Sub-Stack (Cart) to optimize its 16 MFC-Units simultaneously. The harvested energy was converted and stored in lithium polymer batteries.

$$U_{\text{MFC-Line(1)}} + U_{\text{MFC-Line(2)}} + U_{\text{MFC-Line(3)}} + U_{\text{MFC-Line(4)}} = U_{\text{MFC-Sub-Stack(n)}}{}_{n=1\text{-}4} \quad \text{Equation 1}$$

2.3. Automated disconnection and reconnection of microbial fuel cell units based on set voltage reversal blocking thresholds

The voltage reversal blocker checked the status of all 64 MFC-Units once an hour to see if the operating voltages were maintained above the set threshold. Depending on the result, the individual MFC-Units remained connected, were disconnected, or reconnected to/from the power generating MFC-Sub-Stack.

There were three different states for computerized automation (i-iii) and programmed to carry out the connection/disconnection handling: (i) MFC-Unit voltages below a set threshold received the command to disconnect from the circuit. (ii) Isolated (disconnected) individual MFC-Units were operated with a fixed external resistance of 1000 Ω (as in initial acclimatization) to allow biofilm healing and/or protection. Electrolyte fluxes remained as under regular conditions and continued to feed nutrients to the biofilms and air-oxygen to the cathodes and by this microbial respiration remained maintained despite reversal and biofilm healing and conservation was ensured. (iii) When voltages during isolation rose above the set threshold, the isolated MFC-Units were reconnected to their MFC-Line after 1 h of isolation, which was considered the shortest disconnection time. Two minutes later, the voltage threshold criteria was checked again to verify the initial stability of the increased voltage level. If the voltage dropped rapidly below the set threshold during these 2 min, the concerned MFC-Unit(s) remained disconnected for the next 58 min what is detailed in the time bar in the center and of the right side in Fig. 3C.

The next level up in the electronic MFC-Stack hierarchy were the MFC-Lines that are shown in Fig. 2 indicated as Line. Their operation was based on a parallel set of four MFC-Units which were not always at the same voltage level presumably due to heterogenous biofilm properties and electrolyte flux anomalies. They were therefore electronically balanced between them to ensure the same properties for all four MFC-Units (Fig. 3B shows four of the ten possible operation states in an MFC-Line). If the voltage of any one of the four MFC-Units fell below the preset threshold, it was automatically disconnected. The other three MFC-Units remained connected and continued to generate power. This disconnection was thought to reduce the power contribution of the affected MFC-Line by <25 %. As a result, the MFC-Sub-Stack was considered in danger of losing power as this MFC-Line became a bottleneck for the stack current. Consequently, if a second MFC-Unit was isolated in the same MFC-Line, the entire MFC-Line was disconnected from the MFC-Sub-Stack and the stack current bypassed until the reversals were resolved (at least three MFC-Units with voltages above the threshold, like State 2 in Fig. 3.

2.4. Allow voltages to reverse deeper and deeper

The highest voltage threshold to block voltage reversals was 50 mV and chosen because the operating voltages of individual MFCs in serial and balanced stacks with MPPT were found to be low, between 100 mV and 400 mV. The experiment was therefore started with a voltage threshold of +50 mV. Power generation at low and negative voltages was investigated by slowly moving the set threshold from +50 mV to the

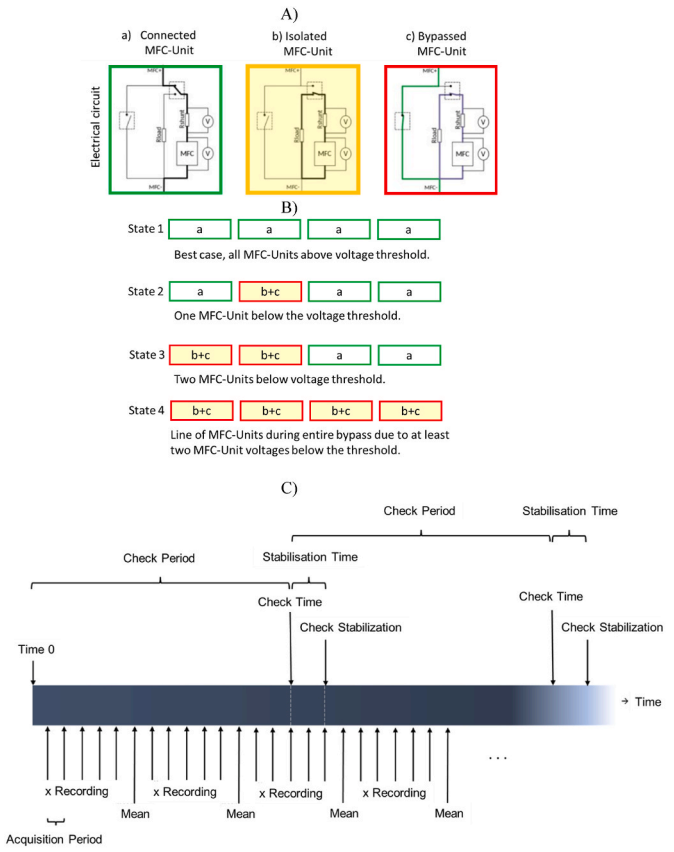

Fig. 3. Detailed MFC-Line states within a serial MFC-Sub-Stack during connection and disconnection of its MFC-Units. A) Three a,b,c control states for individual MFC-Units under automatic voltage reversal blocking. (a) MFC-Unit in power generation mode. (b) Isolation circuit of MFC-Unit with voltage reversal problem (R_{load} = 1000 Ω). (c) Bypass of an MFC-Unit. B) Global view of typical on/off states (1–4) in MFC-Lines. State 1: All units connected. State 2: One MFC-Unit isolated/bypassed. State 3: A second MFC-Unit has been isolated/bypassed. State 4: All MFC-Units are bypassed/isolated in case two become isolated/bypassed. For States 2 and 3 other variants are possible too (not shown). C) On/off regulation of an MFC-Unit that was performed with all 64 of the stack. The parameters were defined by the operator and usually set as follows: Check Time = 60 min to control threshold voltage criteria, Stabilization Time = 2 min to check if on/off decision was justified otherwise it was adjusted. Acquisition Time was 1 min, five Recordings were calculated as a Mean, which was stored in a data file on the central computer along with current and time information.

unwanted −50 mV (using maximum power tracking at the same time). This was done to observe the limits and possible resilience of the voltage inverted MFC-Units in relation to power generation. The theoretically lowest allowed setpoint was zero volts, as below this point power is lost proportionally if there is no compensation for what can be assessed for the voltages with Eq (1). The aim was to find the optimum blocking threshold for the best power generation. It would show how much uncontrolled stack balancing is just an oscillation without power loss in the circuit and how much it is a problem for the biofilms. This oscillation was not always a clearly negative occurrence, as seen from recorded data as shown in Fig. 4A on the right side where the four oscillating curves seem to be in many cases in counterbalance with each other. Here the voltage inversions were allowed to fall lower and lower in a controlled manner. This threshold testing experiment started with the 1000-L MFC-Stack in year two. The reactor was previously in continuous use for 16 months whose process time is found in Table 1, which shows the time context and principal operations in the three years experiment. At the transition stage to year two, it was concluded that the MFC stack needed to be overhauled as the reversals became ever more pronounced what is well visible in Fig. 4A for the days −50 to zero. Computerized voltage reversal blocking and prevention was newly initiated and continued for 189 days into the second year to understand its ability to balance the MFC-Stack (Fig. 4B shows the enforced equilibrium that can be achieved by cutting off inverted MFC-Units). The voltage blocking threshold was lowered from 50 mV in monthly steps of 25 mV, eventually reaching −50 mV after more than six months. On the last day (day 224) of threshold limited reversals, the voltage reversal blocker was disabled, and MFC-Unit voltages were allowed to drop even further for the coming months. The following third year, the experiment was repeated, this time starting at the lowest threshold used before, −50 mV, and then it was increased in 25 mV steps to finally reach +50 mV.

3. Results and discussion

3.1. Microbial fuel cell stack balance by launching the voltage reversal blocker

The first time the electronic voltage reversal blocker was in constant function a balance was established. This event is indicated in Table 1. It shows equally all other experiments conducted during three years of processing. At this initial moment of reversal blocking an existing deep voltage reversal of at about −200 mV with MFC-Line 1 in MFC-Sub-Stack 1 was resolved and remained at 50 mV (in Fig. 4B, this automatic regulation can be seen from day 35 onwards in constant use). The initial voltage adjustment was not that fast established in all cases. In some of the other MFC-Lines it took several days for the voltage reversal to be resolved to the wanted threshold level. Subsequently, the device immediately blocked any voltage reversals that occurred. This was possible because the blocker checked the reversal status on an hourly basis. This resulted in chopped voltage curves until the voltage reversal trend disappeared as shown in Fig. 4B and C for MFC-Units and MFC-Lines (Figs. S5 and S8 show this in more detail). The chopped voltage curves were present in all affected MFC-Units and MFC-Lines when they undercut the set threshold voltage. By setting the cut-off to +50 mV, the apparent voltages of the well-functioning MFC-Lines 2–4 (Cart 1) dropped from 800 mV to 700 mV as in Fig. 4B, see days ~20–40. These drops corresponded approximately to a voltage compensation within the circuit in the same MFC-Sub-Stack as Eq (1) suggests. Voltage reversal prevention was demonstrated at an early stage and further work was then possible to investigate under what conditions the voltage blocker enabled optimum power generation. Stack currents were visibly less affected by MFC-Unit isolation what can be seen in the detailed current curves in Fig. 6B. The initially expected bottleneck for stack currents did not appear in an obvious manner. In conclusion, voltage reversal blocking from an uncontrolled state usually improved MFC-Stack balance.

3.2. Voltage reversal blocking versus no regulation

The voltage reversals were monitored for three years (Fig. 4A–C) while the 1000-L MFC-Stack was fed with municipal wastewater. In two extended half-year periods, electronic voltage reversal blocking experiments were performed. In both experiments the MFC-Stack was in a critical state of advanced ageing after one and later two years of previous use which is visualized in the event Table 1. In both blocking experiments of > six months, the novel blocking device made a difference by enabling a balanced state to be achieved what increased power output. Prior to this first reversal blocking experiment, no voltage reversal control was performed for 16 months (Fig. 4A). Voltage reversals were not a pressing issue initially, but reversals became more frequent and intense towards the end of the first year after inoculation and became most intense in the days −50 to zero as Fig. 4A shows, what was expected and had been seen before [49]. During this unregulated phase, voltage reversals were often compensated by voltage increases in other units as visible in Fig. 4A and later in Fig. 4B and C during

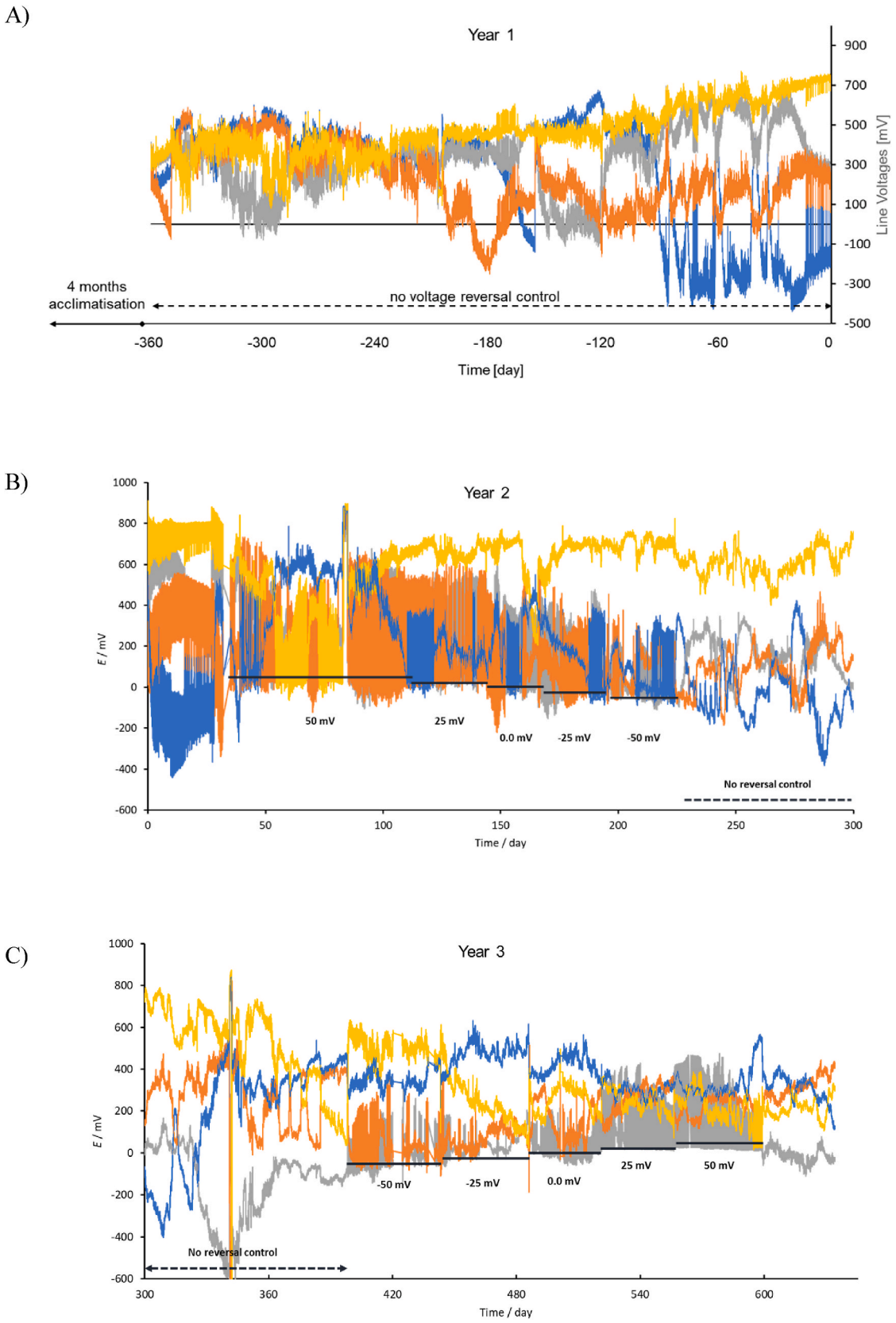

Fig. 4. MFC-Line voltages in MFC-Sub-Stack 1 over three years of processing. A) MFC-Stack for the first year before voltage regulation started (adapted with permission [11]). B) Start of voltage reversal blocking in second year with set voltage thresholds for disconnection and reconnection of MFC-Units for > six months followed by no control. C) Voltage reversal blocking in the third year of voltage reversal blocking for > six months. Thresholds setting in the opposite order to (B) during the same seasons, winter to summer. Color code for MFC-Lines according to Fig. 1: blue 1, grey 2, orange 3, yellow 4 (MFC-Line = parallel connection of four MFC-Units). The threshold experimental voltage data were averaged to 10 min, higher averaging would blur the important to notice trespassing reversal signals below the blocking threshold (for a more detailed view, see supplementary information with many detailed Figures in S5).

Table 1
1000-L MFC-Stack experiments performed over three years with no major process interruption at the wastewater treatment plant Chateauneuf Sion in Switzerland. Voltage reversal management and serial/parallel stack balancing were performed in years two and three (green and orange). Phase 2 is the focus of the voltage reversal work reported in this study.

Year	Phase	February	March	April	Mai	June	July	August	September	October	November	December	January
0	0	Construction and installation of 1000 liter MFC-Stack								Acclimatization			
1	1	Maximum power point tracking (MPPT), no voltage reversal blocking [11]											
2	2	MPPT and voltage reversal blocking with cut-off thresholds decreasing from +50, +25, 0, -25, -50 mV								MPPT no voltage reversal blocking			
3		MMPT and voltage reversal blocking with cut-off thresholds increasing from -50, -25, 0, +25, +50 mV								MPPT, no voltage reversal blocking		End of experiment	

unregulated periods. The proposition of entangled oscillations was supported by the observation that power generation did not seem to be affected by the reversals, which is in line with the theory of Kirchoff's Voltage Law that corresponds to Eq (1). However, at MFC-Unit level, the compensation was not always obvious due to the electronic design, as 16 MFC-Units were in use, connected in parallel and in series. There were instances where voltage regulation would have been beneficial, as there were voltage drops and no voltage rise in other MFC-Units to compensate for this drop, what indicated that power was lost due to this voltage reversals. It was intended to avoid such reversals by the use of a voltage reversal blocking algorithm as detailed in Fig. 3C resulting in measurable power increases as depicted in Table 2.

MFC-Sub-Stack 1 was the best performing of the four MFC-Sub-Stacks 1–4. It was the ideal section of the MFC-Stack to monitor voltage reversals and blocking effects. The same phenomenon was observed in the MFC-Sub-Stacks 2–4, where the COD was lower due to the progress in wastewater treatment. Therefore, in these later sections of the MFC-Stack, other bioconversions were present in addition to

Table 2
Average power during voltage blocking experiments with specific voltage thresholds changed once a month (see Fig. 4B and C for timing and other details of threshold application). A) First experiment in the second year of MFC-Stack effluent treatment. B) Inverse experiment, where the set thresholds were increased at approximately the same rate as the previous year.

A) Controller Setting Changes ------>	No Threshold				At 50 mV				At 25 mV				At 0 mV				At -25				At -50				No Threshold			
	Average Power [mW]																											
MFC-Sub-Stack	1	2	3	4	1	2	3	4	1	2	3	4	1	2	3	4	1	2	3	4	1	2	3	4	1	2	3	4
Line 1	-12.2	2.8	1.8	0.2	20.9	24.2	7.3	2.5	5.3	2.8	0.1	0.1	8.2	6.9	0.1	0.0	4.8	0.6	0.1	0.0	0.8	-0.5	0.0	0.0	0.5	-1.1	-0.7	-0.3
Line 2	12.3	0.0	3.9	0.6	9.9	6.7	15.5	11.2	2.9	5.9	7.1	0.5	0.9	1.5	0.2	0.0	0.4	6.2	0.3	0.0	0.3	5.4	0.5	0.1	2.8	3.8	1.6	0.3
Line 3	7.1	0.3	-0.9	0.9	3.5	9.8	3.9	5.7	1.9	10.1	1.2	0.1	2.2	2.6	0.2	0.0	2.9	0.8	0.2	0.0	2.1	4.7	0.3	0.0	0.4	2.8	0.5	0.2
Line 4	20.3	5.3	0.8	1.5	16.2	1.2	3.3	5.3	26.6	5.0	7.5	0.1	23.0	5.3	0.1	0.0	21.4	8.5	0.3	0.0	15.7	6.0	0.3	0.1	10.4	2.2	1.1	0.5
Stack Total	27.5	8.4	5.6	3.2	50.5	42.0	30.0	25.0	36.7	23.9	15.8	0.8	34.4	16.3	0.7	0.0	29.4	16.1	0.9	0.0	18.9	15.6	1.1	0.0	14.1	7.7	2.4	0.7
1000-L MFC-Stack Total	44.7				147.5				77.2				51.4				46.4				35.6				24.9			

B) Controller Setting Changes ------>	No Threshold				At -50 mV				At -25 mV				At 0 mV				At 25				At 50				No Threshold			
	Average Power [mW]																											
MFC-Sub-Stack	1	2	3	4	1	2	3	4	1	2	3	4	1	2	3	4	1	2	3	4	1	2	3	4	1	2	3	4
Line 1	7.1	5.0	0.3	0.1	7.6	5.4	0.4	0.3	6.6	6.8	0.3	0.1	8.6	3.0	4.1	0.1	6.1	1.7	4.1	0.0	6.4	0.5	3.4	0.0	5.7	-3.6	0.3	0.0
Line 2	-1.7	4.5	0.4	0.0	-0.4	1.6	0.4	1.0	0.4	8.9	0.4	-0.1	0.1	13.2	12.9	0.1	0.3	10.2	12.0	-0.9	0.1	10.4	6.2	0.0	-0.1	5.6	0.5	-0.1
Line 3	4.6	0.9	0.3	0.1	0.1	4.2	0.4	1.8	0.8	2.7	0.2	0.0	3.2	10.2	11.8	0.1	5.1	6.4	2.4	0.0	5.3	3.0	0.4	0.0	5.5	6.1	0.2	0.0
Line 4	5.1	2.6	0.0	0.0	11.3	3.2	0.4	0.8	3.8	-2.0	0.0	0.0	5.3	5.1	-0.5	0.1	5.1	6.2	2.3	0.0	4.2	6.1	0.4	0.0	3.8	3.7	0.1	0.0
Stack Total	15.1	13.0	1.0	0.2	18.7	14.4	1.6	3.9	11.6	16.5	1.0	0.0	17.2	31.5	28.3	0.3	16.7	24.5	20.8	0.0	16.0	20.0	10.4	0.0	15.0	11.8	1.2	-0.1
1000-L MFC-Stack Total	29.3				38.6				29.1				77.3				62.0				46.4				27.9			

energy production, such as the removal of nitrogen, sulfur and trace compounds [11].

3.3. Automatic on/off switching of microbial fuel cell units

The smallest controlled unit in the electronic hierarchy of the 1000-L MFC-Stack was the 16-L MFC-Unit. It remained functional as designed during repeated on/off switching, as indicated by the voltage and current curves in Fig. 5A and B. The online voltage data was sufficient to regulate, balance and optimize the power generation of the MFC-Units. When the voltage dropped below the pre-set threshold, the MFC-Unit was automatically disconnected, and the inversion of the voltage was blocked. The automatic on/off control of the MFC-Units prevented voltage reversals in most cases. During isolation, the anode and cathode were directly connected across a 1000 Ω external resistor and the MFC-Unit voltage rose rapidly to >600 mV pseudo-open circuit voltages (p-OCV) as seen for four voltage MFC-Unit curves in Fig. 5a. This isolation reduced the current by an order of a magnitude but still allowed continuous microbial respiration, which was the objective and is plotted in Fig. 5b, there are more details in Fig. 5c, following the arrow. The now lower respiration rate was similar to that used to acclimatize the 1000-L MFC-Stack initially. The fixed load (1000 Ω) was well above the usual internal resistances of weak MFC-Units. In general, the internal resistance of a well-functioning MFC-Unit was between 15 and 40 Ω [11]. In addition to biofilm degradation, there are many other reasons for increased resistance, such as temporarily lower COD due to dilution from heavy rainfall [50], locally reduced electrolyte fluxes, or changes in oxygen supply and concentration. The isolation period of at least 1 h provided a window to read the anode potential derived from the OCV of the isolated MFC-Units. These approximate anode potentials indicated that, in most cases, the observed imbalances with MFC-Sub-Stacks were not in obvious correlation with the perceived weakness of the biofilms. It confirmed that imbalances were often due to causes other than biofilm weakness. This was evidenced by the fact that reversals were resolved in a rapid transition rather than a gradual process what was unexpected and perceived as a novel observation. In contrast, biofilm growth to restore sufficient function was seen as a rather slow process [51].

Overall, voltages and currents of isolated MFC-Units increased during the automated hourly isolations as shown in Fig. 6A as rising plateau peaks for voltages and similar for currents in Fig. 5c as well visible during the hourly off-times. The current increases during isolation were an indication that the electrogens were respiring under the healing/acclimatization regime despite the external resistor who had to slow the respiration/current rate. The improvement in voltage and current continued when the isolation lasted longer than an hour as it can be seen in Fig. 5a with a series of rising plateau peaks and currents that increased from very low levels as in Fig. 5c. In fact, it sometimes took a long time for a sufficient working voltage to be achieved and for the MFC-Unit to be definitively reconnected to the MFC-Sub-Stack circuit as shown in Fig. S5 with extensive details.

The automatic isolation resulted in most cases in two chopping patterns of the voltage curves in relation to the severity of the voltage reversal trends (i, ii): (i) There was the voltage curve with a comb-like appearance as in Fig. 6A, see the first row, where Units1-4 show this phenomenon during repeated off times, starting with an instantaneous steep voltage rise and reaching then a peak value at a slower rate towards the end of the blocking hour what can be seen in Fig. 6A, beside the first row it was also appearing in the third row on this Fig. 6A. This was followed by a steep voltage drop on automatic reconnection to the stack. Next was a low working voltage which continued for another hour. This 2-h pattern was repeated several times before a reversal resolution. (ii) The second type of chopped voltage curve resembled a chain of teeth curve where the next period of isolation repeated itself immediately without an hourly reconnection in between as Fig. 5a shows simultaneously for four MFC-Units in an MFC-Line. This pattern resulted from a stronger voltage reversal trend forcing a longer MFC-Unit disconnection, as the MFC-Unit voltages were only slowly recovering to the required level. This second teeth-like voltage curve signature usually lasted for several hours or even days what can be found in Fig. S5 in all its variants. The isolation status in both types of chopped curves lasted until final reconnection to the stack became possible, whose transition was often instantaneous for both curve types. This indicated that electrotechnical phenomena in the MFC-Sub-Stack were more relevant to the presence of voltage reversal trends than the biofilm properties. Beside this, there were other rarer and less obvious voltage curve patterns than the two described what can equally be found in the multipage Fig. S5. Voltages that change in only 2 h were seen before [27] and found to not originate from biofilm growth [52] what was in line with the results found here.

The comb-like on/off mode (i) gave the biofilms a full respiration window every hour before the next slower respiration hour was repeated due to the renewed isolation what is well visible in the first row of voltage curves in Fig. 6. This alternation was seen to be beneficial to keep the electrogens in sufficient anaerobic respiration while preparing for sustained recovery from the voltage reversal trend and a stable reconnection of the MFC-Unit to the MFC-Sub-Stack became possible.

Conversely, with prolonged MFC-Unit isolation (ii), respiration was reduced constantly as the MFC-Units which remained isolated without

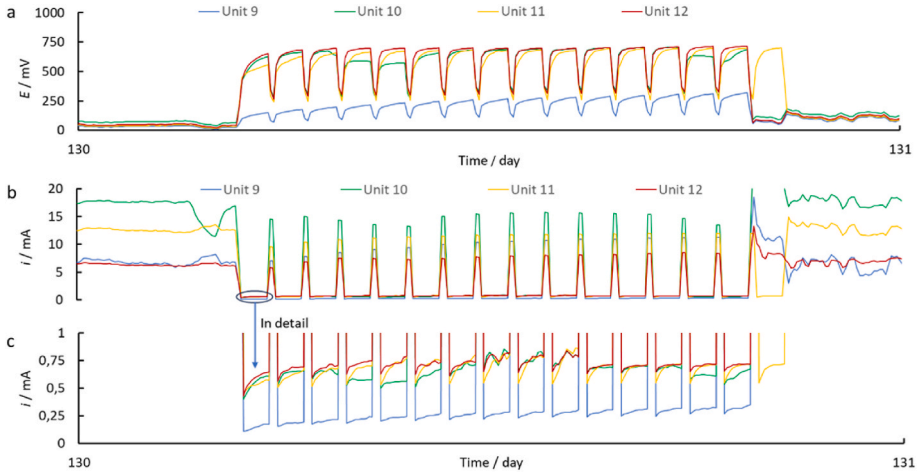

Fig. 5. Chopped voltage and current curves (chain of teeth voltage curve) at a blocking threshold of 25 mV. a) MFC-Unit voltages of an MFC-Line in isolation. b) Current curves during MFC-Line isolation. c) Details of MFC-Unit currents in b) during isolation. The currents increased slightly in all cases, although the pseudo-open circuit voltage increased, indicating that biofilm healing was possible if required.

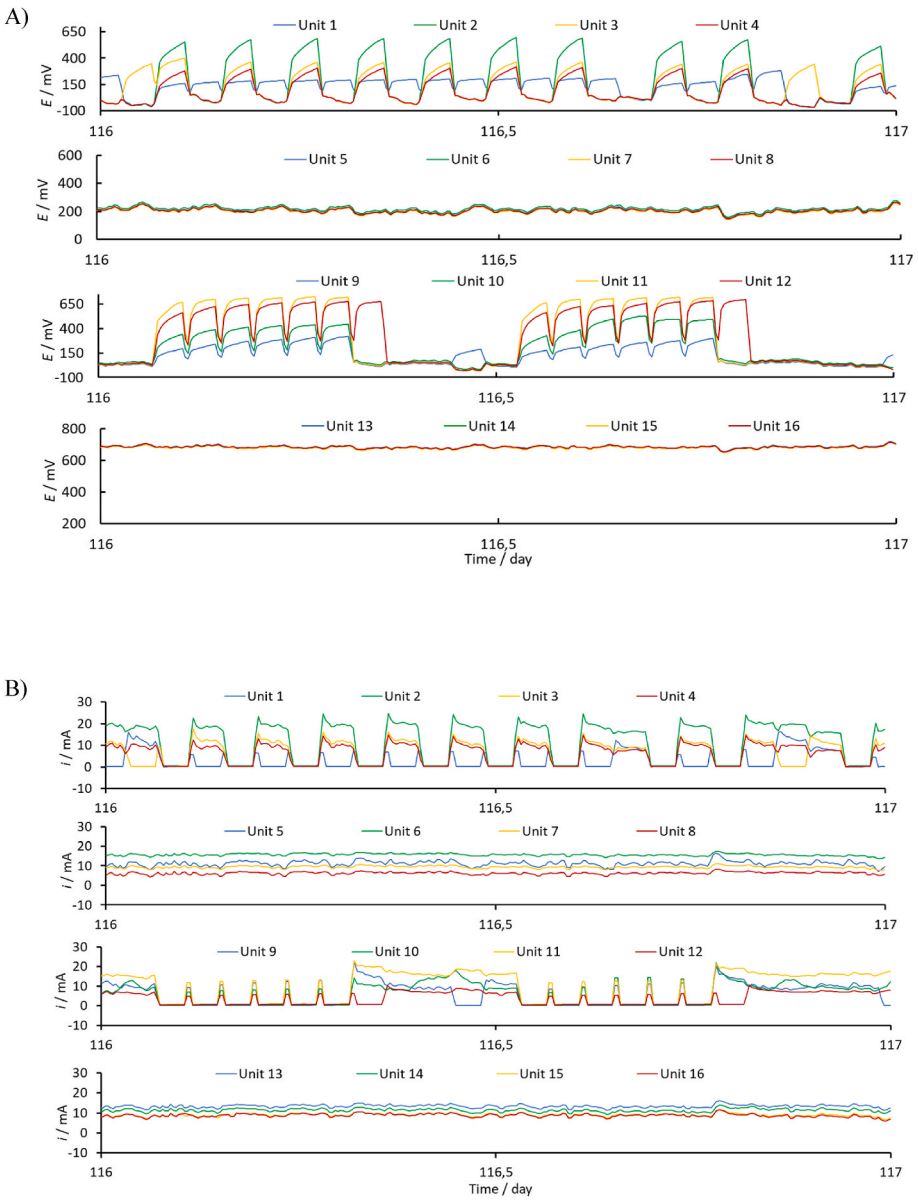

Fig. 6. Voltages and currents of all MFC-Units in the MFC-Sub-Stack-1 under voltage reversal control during one day. A) 16 MFC-Unit voltages of four MFC-Lines showing the single and multiple isolation states to prevent reversals. Curve types: comb = MFC-Units 1–4 (MFC-Line 1), teeth = MFC-Units 9–12 (MFC-Line 3). MFC-Line 2 (MFC-Units 5–8) is visibly not affected, and MFC-Line 4 (MFC-Units 13–16) is shifted to a higher voltage by the voltage reversal trend despite blocking at 25 mV what is in line with Kirchhoff's rule for electrical circuits. (B) Currents during on/off switching as in A for the same MFC-Units. The blocking threshold was set to 25 mV at this time. Bypass currents on the unit level are the currents that are not close to zero in cut-off moments, see top and third row of current curves in (B).

intermittent reconnection what is seen in Fig. 5A as close chain of closely following plateau peaks. Here the biofilms were thought to be weaker and/or at greater risk of losing more of their electrogenic properties. Nevertheless, the isolation mode with the re-acclimatization regime was beneficial to reach a recovery state that allowed reconnection to the stack. Specifically, a very weak biofilm would recover over time from the chain of teeth-like voltage curves in Fig. 6A, see there the Units 9–12. The improvement process should pass through the comb-like curve type state as in Fig. 6A (Units 1–4) and finally recover completely and then remain connected to the MFC-Sub-Stack, but this systematic was not often seen.

3.4. Automatic on/off switching of microbial fuel cell lines

The 3-m-long MFC-Lines were in fact dual-chambered microbial fuel cells. This setup minimized the number of electronic circuits and components needed and lowered the cost of the setup. The internal electronic organization was designed to be flexible and to cope with the complexity of maintaining a stable voltage across the 3-m long MFC-Line as seen for the two years examination period in Fig. 4B and C. The summed voltages of four MFC-Lines in series were high enough to charge lithium polymer batteries. The main difficulty was that the closed-loop MFC-Line voltage data did not accurately reflect the real MFC-Line voltages. This was explained by Eq (1) and these voltages were called apparent voltages as their data was not real in terms of the electrode potentials of the MFC-Units. MFC-Line and MFC-Unit voltages were not considered to be very useful for controlling the voltage reversal blocking function. However, once the equilibrium was reached, these voltage values were much more in line with the direct real voltage information required, and it was therefore correct to use voltage data that were not adjusted to reality to equilibrate the MFC-Sub-Stacks.

The MFC-Line voltages were made up of its four MFC-Unit voltages

and should have been the same for all of them. However, small differences in the working voltages were recorded what should not be the case. The differences were thought to be caused by different source potentials due to uneven biofilm properties, and most likely due to COD gradients, although no such systematic was clearly identified. In addition, the cathode is a component that influences voltages to some extent too. These differences were particularly apparent when all four MFC-Units of an MFC-Line were isolated, and the stack current was bypassed as Fig. 3Aa shows the individual MFC Units switch mechanism and there are bypass currents seen in Fig. 6B. It was thought that the MFC-Line voltages could be balanced by regulating the voltages at the MFC-Unit level. It was possible to balance the MFC-Lines within themselves by electronically switching their MFC-Units on and off. This balancing was done in relation to the set threshold working voltage and the voltage status of the neighboring MFC-Unit, while the apparent voltage of the MFC-Line was not taken into account in this balancing work. When the balance was lost due to a starting reversal in one of its four MFC-Units, the affected MFC-Unit was automatically isolated. The three remaining MFC-Units stayed connected to each other and to the MFC-Sub-Stacks named State 2 in Fig. 3B. Often, after isolating a single MFC-Unit, a second MFC-Unit in the same MFC-Line would be reversed, switched off and isolated. This happened frequently because its voltage situation was often similar to the first isolated MFC-Unit, as it was systemically intended to be like that by the digital voltage reversal control procedure. In addition, all parallel MFC-Units should theoretically have the same voltage, but in isolation it became clear that there were external factors such as biofilm characteristics and flux differences that most likely caused parallel MFC-Unit electrodes to not automatically have the exact same characteristics. The second disconnection of an MFC-Unit that is reached in Fig. 3B as State 3 indicated the beginning of a disbalanced MFC-Line and to prevent this all four MFC-Units of this MFC-Line were disconnected and isolated as seen Fig. 3B being State 4. This was done to prevent an increasing misalignment of the MFC-Unit characteristics within the MFC-Lines. It also permitted to avoid a stack current bottleneck with the unwanted negative effects on power generation, microbial growth and stress.

Despite successful balancing, the high and low voltage trends of the apparent voltage curves of the serially stacked MFC-Lines remained stable over long periods of time, in fact over many months when considering noncontrolled phases in Fig. 4B and C. Even during voltage reversal blocking, negative apparent voltage trends did not stop. The reasons for the lack of spontaneous adaptation and the attainment of equilibrium under reversal control could not be fully investigated due to the length of time required. However, the most likely causes were the specific conditions of the MFC-Line and other reasons affecting the apparent voltages of the MFC-Line [53]. The influences on the electrical circuits included uneven electrolyte flow, particle sedimentation, salt deposition and other unidentified causes that influence mass transfer to the biofilms. MFC-Line 4 in the MFC-Sub-Stack 1 was exemplary for a high line voltage curve that remained at this elevated level for a long time as seen in Fig. 4A–C for the days −180 to 400. The high voltage curves themselves were in fact a mirror for the out-of-control voltage reversal trends.

3.5. Lowering the voltage threshold to allow gradually deeper and deeper voltage reversals

In order to understand the dynamics and find the best cut-off threshold for voltage reversal blocking, the allowed voltage threshold of the blocker was lowered in monthly steps until it passed the zero-volt threshold where voltage reversal begins what is reached in the middle of Fig. 4B. Further reduction below the zero-volt threshold was therefore not advisable [54]. Nevertheless, the set voltage was lowered below this point to understand to what negative level the computerized method was effective and how long the biofilms remained functional. Moreover, in the case of compensatory voltage shifts the power should remain unchanged even with reversals but this was not observed in the time frames examined as the data in Table 2 show.

The voltage reversal control in voltage decreasing experiment started at a reversal blocking threshold of +50 mV as seen in Fig. 4B on the left side with day 35. It was then lowered in monthly steps of 25 mV to finally reach −50 mV. The whole process took more than six months, which allowed to observe the effect on power output as found in Fig. 7A. As the threshold was lowered, deeper voltage reversals occurred, and power was reduced what is shown with detailed numbers and their summaries in Table 2A. The gradual loss of power was not linear. Above the zero-volt threshold it was more significant with 48 % from 50 mV to 25 mV and 33 % from 25 mV to zero volt. Below the zero-volt threshold it was 10 % and 23 %, what was calculated from Table 2A values, and with the transition to no control there was again a 30 % loss.

With deeper voltage reversals, it was expected that biofilms would suffer and be damaged what has been observed before [42] but not verified here as specific experimental planning is needed to obtain accurate data. Nevertheless, the pseudo-open circuit voltage data confirmed this, what can be seen in global but detailed fashion in the Figure series S5 but remained indistinguishable from biofilm ageing. From an electrical point of view, the power decrease was in accordance with the theory of Kirchhoff's law. Spontaneous inversions recoveries were also observed in the first year in Fig. 4A at all times and in Fig. 4B and C during the uncontrolled periods. These voltage improvements were possible according to Eq (1). All such intermittent voltage reversal resolutions in the absence of the reversal control mechanism were short lived before they dropped back and became negative voltages (see also days 247, 267, 298 and 316 in Fig. 4B and C). Even with the computerized process, voltage reversals were not blocked in an absolute manner what can be seen in Fig. 4B where some short term intermittent deeper voltage drops below the blocking thresholds were possible. This effect remained under control, as it was always the same degree of undercutting the threshold but the negative impact on power generation remained in the low percentage range (see the single digit percentage of trespassing in Fig. 4B). The average powers under specific voltage thresholds and the cutoff frequency were equally assessed as represented in Fig. 8B and in more details in Table 2. Overall, the systematic lowering of the voltage thresholds showed that the best performance was obtained despite the highest voltage threshold used as to be seen in the 50 mV threshold region on the left side of Fig. 7A and in Fig. 8B with the highest bars for any threshold applied. However, this result was challenged in a similar experiment one year later.

3.6. Reactivating the voltage reversal blocker after months without control

On reaching the third year of MFC-Stack processing without interruption, a reactor overhaul was considered as the year before. Without voltage reversal blocking the MFC-Stack had reached the lowest power generation status in four months as visible in Fig. 4C and 7B, days 368–398). This low power situation continued until the end of the second year of effluent treatment. The average power was now five times lower than the best recorded value at stack balance what is detailed in Table 2B.

Nevertheless, the average low power did not change in the event of a significant unfolding voltage reversal. This showed that intense oscillations are well possible at all times due to electrotechnical reasons. This was in an exemplary fashion observed with the negative voltage of MFC-Line 2. There it reached the lowest voltage in this work, respectively the worst reversal of −600 mV that is shown Fig. 4C, during the days 338–345. This very negative voltage was possible because it was a stack of four MFC-Lines where each MFC-Line in the stack has the potential to amplify this value. Negative voltages have been observed before in a two-unit MFC-Stack with a total volume of 170 mL [55] and in similar negative values were recorded in a 12 L quadruple pilot MFC-Stack [42].

The 1000-L MFC reactor was considered in this third year of processing at the end of its life, needing maintenance. Conversely, as in the

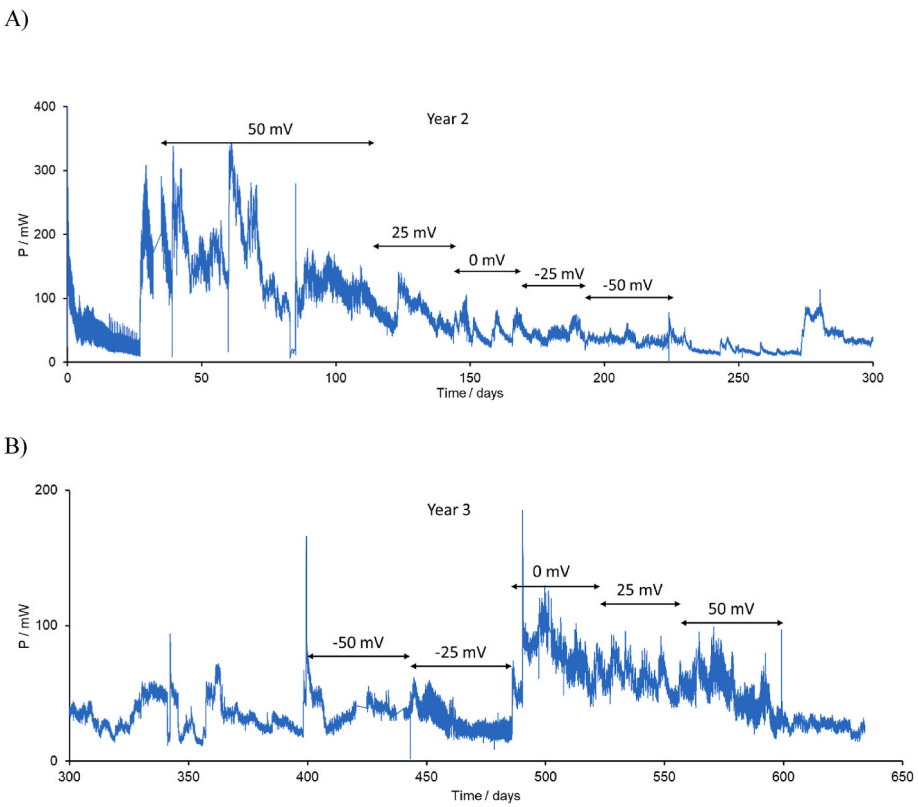

Fig. 7. Power of the 1000-L MFC-Stack in the second and third year of processing. A) Applying descending voltage reversal thresholds in the second year of processing. B) Resulting power in the third year of processing with > six months of increasing voltage reversal blocking thresholds. Average powers at the specific voltage reversal thresholds were calculated and are found in Table 2.

previous year, this reactor status provided the opportunity to test the voltage blocker in a very challenging situation. The voltage reversal blocker was therefore relaunched to understand if it had the ability to upregulate the low voltages of the MFC-Stack and improve power output. To carry out this experiment in a systematic and comparable manner as the decreasing voltage experiment in the second year that is shown in the left part of Fig. 4B, it was started in the same winter month as in the previous second year of processing. However, this time the reversal blocker was set to a starting threshold of −50 mV first, and then the threshold was increased by 25 mV per month over the next six months. Setting the first threshold at −50 mV, power increased by 32 % compared to the no control situation before starting what is detailed in Table 2B. After a further increase of the threshold to −25 mV, the initial power gain was lost what is visible from the summaries for these two conditions in Table 2B. This loss was attributed to the fact that voltage reversal control was realized at a low threshold and unhindered voltage oscillations remained more important than the low range of control. Blocking at the next higher level at zero voltage improved the power by 266 % (77.3 mW). After two further threshold increases to 50 mV, some power was lost again, falling back by 40 % (46.4 mW). The details/numbers of this somewhat unexpected result are found in Table 2B. Overall, the results of this third year of threshold variation experiments showed that the highest power of the 1000-L MFC-Stack decreased in a year by 48 % due to ageing. It was also seen that the performance recovery was more a function of the second and the third MFC-Sub-Stack, which contributed well, while the first and fourth did not contribute to this performance recovery. Overall, the 12 m length of the reactor and the treatment protocol applied cleaned the effluent still rather well with an average COD removal of 80 % during voltage reversal control experiments what Fig. S4 shows, and this in the third year of reactor use. This sustained cleaning capacity despite aging is in fact a promising observation. It indicates that the method works, even after three years of processing. The persistent cleaning effect is helpful for the needed redundancy with this kind of large microbial fuel cells.

3.7. *Voltage curves contracted under voltage reversal blocking*

As the voltage reversal blocker achieved automatic balancing of the serial MFC-Sub-Stack 1, the voltage curves contracted as indicated in Fig. 4B and C, this in periods of reversal control with the characteristic voltage threshold curves. Contraction means that here the four voltage curves in the quadruple serial stack came closer together above the threshold voltage depending on the restriction level the controller exercised by enforcing the predefined voltage cut off threshold. The voltage of these lines reached a realistic and not just apparent working voltage, and no outlier voltages were recorded anymore. The best power generation, according to Table 2, correlated with all MFC-Lines 1–4 operating voltages in the same range as seen with the MFC-Sub-Stack 1 visible in Fig. 4B and C, days 35–114 and 486–521. Based on this dynamic, there was no need to specifically control the higher MFC-Line voltages, as their levels were entangled across the electrical circuit and descended to the desired realistic voltage level that can be seen in Fig. 4B and C. This favorable voltage adjustment was an electrotechnical effect and could be explained by the dynamics within the serial electrical circuit used and follows Kirchhoff's law for voltages in electrical circuits that can be calculated with Eq (1), which helps to understand the dynamics of various interconnected voltage levels in this work. The shrinking amplitudes of the voltage curves due to the electronic control of the reversal blocker was observed at all electronic levels of the 1000-L MFC-Stack with variable usefulness for MFC-Stack reversal by computerized control. The following three differences were observed in (i) MFC-Units, (ii) MFC-Lines and (iii) MFC-Sub-stacks. (i) For individual MFC-Units, negative voltages were blocked at voltage thresholds. This resulted in a voltage upshift for negative voltage curves, which was

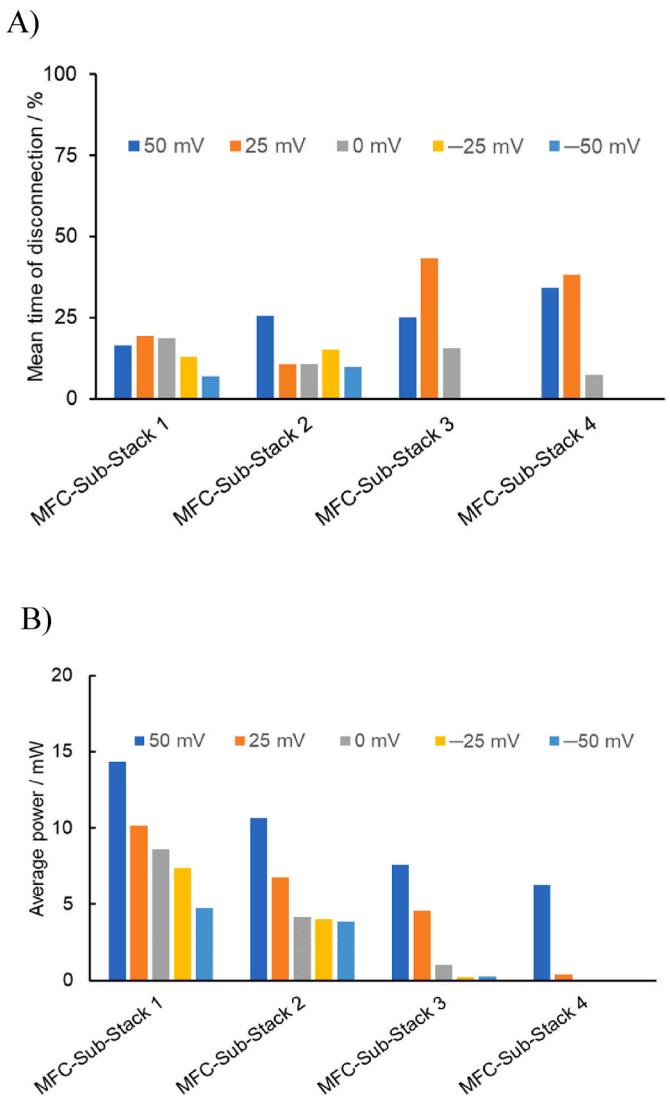

Fig. 8. A) Length of reversal blocking or time of disconnection of MFC-Units from their MFC-Sub-Stack in experiments with descending thresholds. Table 1 shows that these data were collected in the second year of processing. B) Average power in correlation to the disconnection frequency in (A).

an important change in terms of voltage curve contraction, while at the same time higher voltage curves >400 mV tended lower. The (ii) MFC-Line voltages without control oscillated visibly as Fig. 4 shows for all three years of processing. In the best-balanced states, the voltages resembled the expected working voltages for single MFCs what is found in Fig. 4B at 50 mV threshold, and in Fig. 4C at zero control level [56]. (iii) The voltage curves of the MFC-Sub-Stack also contracted but provided less insight into the mechanics of voltage reversals and balancing than the MFC-Units. This was because this voltage was a combination of 16 MFC-Unit voltages connected in series and in parallel whose details are found in the upper part of Fig. 2. Overall, the contraction of the voltage curves was in line with the achievement of stack balance, which allowed at the same time the best power generation.

4. Conclusions

Long-term operation of large microbial fuel cells is possible. One to two years are the time frame seen here to control power generation levels. In the third-year power generation was reduced by at least 50 %. The new electronic voltage reversal blocking device with its healing mode proved to be not only useful to prolong service life but also as a tool for balancing a large serial MFC-Stack. From the first moment of controller use, voltage reversals disappeared either quickly or relatively soon afterwards. The blocking effects were accurately regulated using online data at the MFC-Unit level. Voltage reversal blocking was effective in combination with maximum power point tracking. These two electronic measures, using the power tracker and the voltage reversal controller, allowed 16 MFC-Units to be optimized simultaneously. MFC-Units that were close to voltage reversal were isolated and continued in protection mode. This supported biofilm protection and healing. Isolated MFC-Units recovered within hours or days. During three years of processing, the MFC-Stack was obviously ageing as no electrode maintenance was carried out, which correlated with an increasing but slow loss of efficiency for power generation. The ageing effect on power generation was suppressed to a good extent with the electronic voltage reversal blocking function, which simultaneously balanced the MFC-Stack. Five levels of voltage thresholds were tested twice, and two different levels correlated with the best power output, one at +50 mV and one a year later at zero volts. The new electronic device increased power by a factor of 1.7–2.7. It is worth noting that improved power generation was possible even from an aged end-of-life 1000-L MFC-Stack, which was in its third year of continuous municipal wastewater treatment. Overall, the electronic voltage regulator successfully blocked voltage reversals in a biocompatible manner. These results should be useful for future work on the scale-up of multi-unit MFC-Stacks. There remains the work on the question of how well long-term stack stabilization will influence the power generation process's effectiveness. Further work is needed to understand how biofilms react to on/off states of MFC-Units. Finally, how much more sophisticated electronic control would improve the power generation process and what is needed for a self-sustaining system on a much larger scale.

Declaration of generative AI and AI-assisted technologies in the writing process

During the preparation of this work the authors used DeepL Write to control grammar, word use and style. After using this tool, the authors reviewed and edited the content as needed and take full responsibility for the content of the publication.

CRediT authorship contribution statement

Sunny Maye: Formal analysis, Investigation, Writing – review & editing. **Louis Delabays:** Software, Investigation. **Jules Sansonnens:** Investigation, Formal analysis. **Maxime Blatter:** Investigation, Writing – review & editing. **Gérald Huguenin:** Supervision, Writing – review & editing. **Fabian Fischer:** Conceptualization, Formal analysis, Writing – original draft, Writing – review & editing, Supervision, Project administration, Funding acquisition.

Declaration of competing interest

The authors declare that they have no known competing financial interests or personal relationships that could have appeared to influence the work reported in this paper.

Acknowledgements

Support from the Swiss Federal Office of Energy (project SI/501573-01), the TheArc Foundation and HESSO Valais. This work was greatly supported by the team of the wastewater treatment plant of Chateauneuf (City of Sion, Switzerland).

Appendix A. Supplementary data

Supplementary data to this article can be found online at https://doi.org/10.1016/j.rser.2024.115017.

Data availability

Data will be made available on request.

References

[1] Asensio Y, Mansilla E, Fernandez-Marchante CM, Lobato J, Cañizares P, Rodrigo MA. Towards the scale-up of bioelectrogenic technology: stacking microbial fuel cells to produce larger amounts of electricity. J Appl Electrochem 2017;47:1115–25.

[2] Huang Y, Zhao Y, Tang C, Yadav AK, Abbassi R, Kang P, Cai Y, Liu A, Yang A, Li M. A glance of coupled water and wastewater treatment systems based on microbial fuel cells. Sci Total Environ 2023;892:164599.

[3] He L, Du P, Chen Y, Lu H, Cheng X, Chang B, Wang Z. Advances in microbial fuel cells for wastewater treatment. Renew Sustain Energy Rev 2017;71:388–403.

[4] Mohyudin S, Farooq R, Jubeen F, Rasheed T, Fatima M, Sher F. Microbial fuel cells a state-of-the-art technology for wastewater treatment and bioelectricity generation. Environ Res 2022;204:112387.

[5] Nawaz A, ul Haq I, Qaisar K, Gunes B, Raja SI, Mohyuddin K, Amin H. Microbial fuel cells: insight into simultaneous wastewater treatment and bioelectricity generation. Process Safe Environ Prot 2022;161:357–73.

[6] Rajesh S, Kumawat AS. Opportunities for microbial fuel cells to utilize post-harvest agricultural residues. Ionics 2023;29:4417–35.

[7] Kusmayadi A, Leong YK, Yen HW, Huang CY, Dong CD, Chang JS. Microalgae-microbial fuel cell (mMFC): an integrated process for electricity generation, wastewater treatment, CO_2 sequestration and biomass production. Int J Energy Res 2020;44:9254–65.

[8] Kumar T, Jujjavarapu SE. Carbon dioxide sequestration and wastewater treatment via an innovative self-sustaining algal microbial fuel cell. J Clean Prod 2023;415:137836.

[9] Rossi R, Logan BE. Impact of reactor configuration on pilot-scale microbial fuel cell performance. Water Res 2022;225:119179.

[10] Opoku PA, Jingyu H, Yi L, Ewusi-Mensah D, Miwornunyuie N. Scalability of the multi-anode plug flow microbial fuel cell as a sustainable prospect for large-scale design. Renew Energy 2023;207:693–702.

[11] Blatter M, Delabays L, Furrer C, Huguenin G, Cachelin CP, Fischer F. Stretched 1000-L microbial fuel cell. J Power Sources 2021;483:229130.

[12] Hiegemann H, Littfinski T, Krimmler S, Lübken M, Klein D, Schmelz KG, Ooms K, Pant D, Wichern M. Performance and inorganic fouling of a submergible 255 L prototype microbial fuel cell module during continuous long-term operation with real municipal wastewater under practical conditions. Biores Technol 2019;294:122227.

[13] Kim T, Kang S, Kim HW, Paek Y, Sung JH, Kim YH, Jang JK. Assessment of organic removal in series-and parallel-connected microbial fuel cell stacks. Biotechnol Bioproc Eng 2017;22:739–47.

[14] Huang L, He J, Jiang C, Weng S, Zhao F, Zhong H, Chen Y. Strategies to alleviate clogging in constructed wetlands: what can be learned from the microbial fuel cell coupled membrane bioreactor? J Clean Prod 2023;405:136973.

[15] Faisal M, Muttaqi KM, Sutanto D, Al-Shetwi AQ, Ker PJ, Hannan MA. Control technologies of wastewater treatment plants: the state-of-the-art, current challenges, and future directions. Renew Sustain Energy Rev 2023;181:113324.

[16] Degrenne N, Buret F, Allard B, Bevilacqua P. Electrical energy generation from a large number of microbial fuel cells operating at maximum power point electrical load. J Power Sces 2012;205:188–93.

[17] Martinez SM, Di Lorenzo M. Electricity generation from untreated fresh digestate with a cost-effective array of floating microbial fuel cells. Chem Eng Sci 2019;198:108–16.

[18] Gajda I, Stinchcombe A, Merino-Jimenez I, Pasternak G, Sanchez-Herranz D, Greenman J, Ieropoulos IA. Miniaturized ceramic-based microbial fuel cell for efficient power generation from urine and stack development. Front Energy Res 2018;6:84.

[19] Song YE, Boghani HC, Kim HS, Kim BG, Lee T, Jeon BH, Premier GC, Kim JR. Maximum power point tracking to increase the power production and treatment efficiency of a continuously operated flat-plate microbial fuel cell. Energy Technol 2016;4:1427–34.

[20] Mukherjee A, Patel V, Shah MT, Jadhav DA, Munshi NS, Chendake AD, Pant D. Effective power management system in stacked microbial fuel cells for onsite applications. J Power Sources 2022;517:230684.

[21] Sugnaux M, Savy C, Cachelin CP, Hugenin G, Fischer F. Simulation and resolution of voltage reversal in microbial fuel cell stack. Bioresour Technol 2017;238:519–27.

[22] Zhao W, Fu W, Chen S, Xiong H, Lan L, Jiang M, Patil SA, Chen S. High-capacitance bioanode circumvents bioelectrochemical reaction transition in the voltage-reversed serially-stacked air-cathode microbial fuel cell. J Power Sources 2020;468:228402.

[23] Aelterman P, Rabaey K, Pham HT, Boon N, Verstraete W. Continuous electricity generation at high voltages and currents using stacked microbial fuel cells. Environ Sci Technol 2006;40:3388–94.

[24] Boghani HC, Papaharalabos G, Michie I, Fradler KR, Dinsdale RM, Guwy AJ, Ieropoulos I, Greenman J, Premier GC. Controlling for peak power extraction from microbial fuel cells can increasee stack voltage and avoid cell reversal. J Power Sources 2014;269:363–9.

[25] Feito RF, Younas T, Dinsdale RM. Evaluation of a comprehensive power management system with maximum power point tracking algorithm for multiple microbial fuel cell energy harvesting. Bioelectrochemistry 2024;155:108597.

[26] Doan C, Sansonnens J, Morgante M, Savy C, Martinet D, Huguenin G, Maye S, Salvo MV, Fischer F. LED algal microbial fuel cell stack balancing conception: electronic voltage reversal blockage, light feed-starvation cycling, and aeration. Sustain Energy Technol Assessments 2023;60:103464.

[27] Kim B, Choi S, Jang JK, Chang IS. Self-recoverable voltage reversal in stacked microbial fuel cells due to biofilm capacitance. Bioresour Technol 2017;245:1286–9.

[28] Cao X, Wang H, Long X, Nishimura O, Li X. Limitation of voltage reversal in the degradation of azo dye by a stacked double-anode microbial fuel cell and characterization of the microbial community structure. Sci Total Environ 2021;754:142454.

[29] An J, Lee HS. Occurrence and implications of voltage reversal in stacked microbial fuel cells. ChemSusChem 2014;7:1689–95.

[30] Agrahari R, Bayar B, Abubackar HN, Giri BS, Rene ER, Rani R. Advances in the development of electrode materials for improving the reactor kinetics in microbial fuel cells. Chemosphere 2022;290:133184.

[31] Naaz T, Kumar A, Vempaty A, Singhal N, Pandit S, Gautam P, Jung SP. Recent advances in biological approaches towards anode biofilm engineering for improvement of extracellular electron transfer in microbial fuel cells. Environ Eng Res 2023;28:220666.

[32] Leininger A, Yates MD, Ramirez M, Kjellerup B. Biofilm structure, dynamics, and ecology of an upscaled biocathode wastewater microbial fuel cell. Biotechnol Bioeng 2021;118:1305–16.

[33] Ishii SI, Suzuki S, Norden-Krichmar TM, Wu A, Yamanaka Y, Nealson KH, Bretschger O. Identifying the microbial communities and operational conditions for optimized wastewater treatment in microbial fuel cells. Water Res 2013;47:7120–30.

[34] Zhao X, Li X, Li Y, Zhang X, Zhai F, Ren T, Li Y. Metagenomic analysis reveals functional genes in soil microbial electrochemical removal of tetracycline. J Hazard Mat 2021;408:124880.

[35] Atnafu T, Leta S. New fragmented electro-active biofilm (FAB) reactor to increase anode surface area and performance of microbial fuel cell. Environ Syst Res 2021;10:31.

[36] Lepage G, Albernaz FO, Perrier G, Merlin G. Characterization of a microbial fuel cell with reticulated carbon foam electrodes. Bioresour Technol 2012;124:199–207.

[37] He Y, Yang J, Fu Q, Li J, Zhang L, Zhu X, Liao Q. Structure design of 3D hierarchical porous anode for high performance microbial fuel cells: from macro-to micro-scale. J Power Sources 2021;516:230687.

[38] Vilajeliu-Pons A, Puig S, Salcedo-Dávila I, Balaguer MD, Colprim J. Long-term assessment of six-stacked scaled-up MFCs treating swine manure with different electrode materials. Enviro Sci: Water Res Technol 2017;3:947–59.

[39] Fricke K, Harnisch F, Schröder U. On the use of cyclic voltammetry for the study of anodic electron transfer in microbial fuel cells. Energy Environ Sci 2008;1:144–7.

[40] Torres CI, Marcus AK, Parameswaran P, Rittmann BE. Kinetic experiments for evaluating the Nernst-Monod model for anode-respiring bacteria (ARB) in a biofilm anode. Environ Sci Technol 2008;42:6593–7.

[41] Hamelers HV, Ter Heijne A, Stein N, Rozendal RA, Buisman CJ. Butler–Volmer–Monod model for describing bio-anode polarization curves. Bioresour Technol 2011;102:381–7.

[42] Fischer F, Merino N, Sugnaux M, Huguenin G, Nealson KH. Microbial community diversity changes during voltage reversal repair in a 12-unit microbial fuel cell. J Chem Eng 2022;446:137334.

[43] Gajda I, Obata O, Salar-Garcia MJ, Greenman J, Ieropoulos IA. Long-term bio-power of ceramic microbial fuel cells in individual and stacked configurations. Bioelectrochemistry 2020;133:107459.

[44] Gupta S, Srivastava P, Patil SA, Yadav AK. A comprehensive review on emerging constructed wetland coupled microbial fuel cell technology: potential applications and challenges. Bioresour Technol 2021;320:124376.

[45] Liang P, Duan R, Jiang Y, Zhang X, Qiu Y, Huang X. One-year operation of 1000-L modularized microbial fuel cell for municipal wastewater treatment. Water Res 2018;141:1–8.

[46] Khaled F, Ondel O, Allard B, Buret F. Voltage balancing strategies for serial connection of microbial fuel cells. Eur Phys J Appl Phys 2015;71:10904.

[47] Kim B, Mohan SV, Fapyane D, Chang IS. Controlling voltage reversal in microbial fuel cells. Trends Biotechnol 2020;38:667–78.

[48] Molognoni D, Bosch-Jimenez P, Suarez J, Della Pirriera M, Borras E. How to balance the voltage in serially stacked bioelectrochemical systems. J Power Sources 2021;491:229576.

[49] Cristiani P, Gajda I, Greenman J, Pizza F, Bonelli P, Ieropoulos I. Long term feasibility study of in-field floating microbial fuel cells for monitoring anoxic wastewater and energy harvesting. Front Energy Res 2019;7:119.

[50] Krieg T, Mayer F, Sell D, Holtmann D. Insights into the applicability of microbial fuel cells in wastewater treatment plants for a sustainable generation of electricity. Environ Technol 2019;40:1101–9.

[51] Liu G, Yates MD, Cheng S, Call DF, Sun D, Logan BE. Examination of microbial fuel cell start-up times with domestic wastewater and additional amendments. Bioresour Technol 2011;102:7301–6.

[52] Chang CC, Kao W, Yu CP. Assessment of voltage reversal effects in the serially connected biocathode-based microbial fuel cells through treatment performance, electrochemical and microbial community analysis. J Chem Eng 2020;397:125368.

[53] Boghani HC, Michie I, Dinsdale RM, Guwy AJ, Premier GC. Control of microbial fuel cell voltage using a gain scheduling control strategy. J Power Sources 2016; 322:106–15.
[54] Kim T, Yeo J, Yang Y, Kang S, Paek Y, Kwon JK, Jang JK. Boosting voltage without electrochemical degradation using energy-harvesting circuits and power management system-coupled multiple microbial fuel cells. J Power Sources 2019; 410:171–8.
[55] Oh SE, Logan BE. Voltage reversal during microbial fuel cell stack operation. J Power Sources 2007;167:11–7.
[56] Rahimnejad M, Ghoreyshi AA, Najafpour G, Jafary T. Power generation from organic substrate in batch and continuous flow microbial fuel cell operations. Appl Energy 2011;88:3999–4004.